INTERNATIONAL JOURNAL OF AUTOMOTIVE AND MECHANICAL ENGINEERING (IJAME)
ISSN: 2229-8649 e-ISSN: 2180-1606
VOL. 18, ISSUE 1, 8601 – 8611
DOI: https://doi.org/10.15282/ijame.18.1.2021.19.0654

ORIGINAL ARTICLE

Predicting Plastic Flow Behaviour, Failure Mechanisms and Severe Deformation Localisation of Dual-Phase Steel using RVE Simulation

A.K. Rana*[1,2] and P.P. Dey[1]

[1]Department of Mechanical Engineering, Indian Institute of Engineering Science and Technology, Shibpur, Howrah -711103, India
[2]Department of Mechanical Engineering, Faculty of Science and Technology, The ICFAI University Tripura, Agartala -799210, India

ABSTRACT – In this work, the von Mises stress and plastic strain distribution of Ferrite-Martensite–Dual-Phase (FMDP) steels are predicted at various stages of deformation. The failure modes and volume fraction effect are identified based on Representative Volume Element (RVE). FMDP steel consists of a typical ferrite-matrix phase, in which martensite-islands are dispersed. Recently FMDP steels are increasingly used to the various car parts in demand. 2D-RVEs are also utilised to predict the orientations effect of the martensite phase in the FMDP steels. Based on the position of the element, the boundary conditions (BC) are given in the RVE of FMDP steel microstructures. The failure modes are examined in the form of severe plastic strain localisation. While the distribution of islands in the microstructure varies, as a result, the deformation inhomogeneity increases with a rise of martensite fraction. The results of numerical computation and the trend of experimental failure shown in the literature are compared. This is signifying that the overall macro-behaviour of FMDP steel, as a consequence of stress-strain partitioning and influence of martensite-island volume fractions (MVFs), can be predicted by the finite element (FE) based 2D-RVE modelling.

ARTICLE HISTORY
Received: 3rd May 2020
Revised:2nd Mar 2021
Accepted: 30th Mar 2021

KEYWORDS
Deformation localisation;
Material inhomogeneity;
Ferrite-martensite-DP steel;
Micromechanical investigation

INTRODUCTION

In recent years, the search and use of new advanced materials have grown in the automotive industry. In the automobile industry, high strength, as well as enhanced formability in thinner thickness sheet metal, are vital for the car components. FMDP Steels are increasingly being used by the automotive industry to reduce vehicle weight while improving passenger safety. DP steels have been successfully used in vehicle parts that fulfil the need for crashworthiness resistance. It principally acts as a crash absorbent constituent that helps to save energy [1]. Previously used automotive materials for low or medium density and lightweight components, for example, various grades of aluminium and magnesium alloys, did not meet these qualifications. Soft matrix and hard island in FMDP steel with a significant combination of improved strength and elongation can meet the requirements of steelmaker and automobile components manufacturer. Recently there has been a huge demand for weight loss in the automotive sector and features to save energy and improve environmental protection as well as passenger safety concerns. To meet these demanding conditions, advanced high-strength steels (AHSS) are developed [1-2]. The FMDP steels are characterised via a ferritic multiphase microstructure with dispersed martensite-islands. These two phases (F-M) steels have an excellent demanding permutation of high strength and good formability to meet the critical requirements of a certain standard. In the two phases, FMDP steels the pliable ferritic-matrix certifies good cold formability, while the island acts as an enhancing strengthen module [3-4]. Macroscopic mechanical properties mainly depend on two factors, namely hard-island and soft-matrix micro-mechanical properties. It also depends on martensite volume fractions (MVFs) and the morphology of the island. The high strength, high volume fraction, fine size of the island and fine grain size of the matrix usually increase the tensile strength of DP steel.

On the other hand, a higher volume fraction of the island phase reduces ductility [2]. Rana et al. examined the influence of MVFs on stress-strain partitioning behaviour under tensile and cyclic loading of DP steels, respectively [5-6]. Typically with a higher percentage of hard-island content, the ultimate tensile stress (UTS) was found to rise in a reduction of uniform elongation [7]. The strength of the ferritic-matrix was generally determined by its configuration and size of the grain in the microstructure [8]. Paul and Mukherjee [9] compared the efficacy of FE simulation via micromechanics modelling that considers the iso-stress, iso-strain and iso-energy conditions of the two-phase FMDP steels. Consistently, DP steel can be made in the course of the inter critical heat treatment of medium or low carbon steels. It possesses a typical microstructure that consists of some specific volume fraction of high-strength phases, such as an island in a matrix of a softer phase known as ferritic phase [10]. These methods are used repeatedly in industrial conditions by (a) controlled cooling after hot rolling or (b) continuous annealing of cold-rolled sheet. A long phase yielding and a high strain hardening rate are characterised by the ferritic-matrix and island contain of the binary phases DP steel [11]. Also, the amount of island contains and island volume fraction expansion caused by phase transformation during production leads to severe

*CORRESPONDING AUTHOR | Amit Kumar Rana | ✉ amit.mme@gmail.com

local stress concentration mechanisms in the AHSS microstructure. Subsequently, understanding the influence of stress - stain state and strain partitioning between phases in the microstructure are of fundamental importance. Various experimental methods or procedures have been explained to illustrate the structure of DP steels at the micro level such as optical and scanning electron microscopy (SEM) [12-13], transmission electron microscopy (TEM) [14], XRD (high energy) and a neutron-diffraction technique [15-16], and electron backscattered diffraction (EBSD) technique [8] are used by different authors and their group.

For improvement of automotive components from magnesium alloy material, Kamal et al. investigated the metal forming process to make near-net-shape components with high casting quality by thixoforming solution technique. The authors examined the effect of plunger speed and solid fraction on automotive parts for better performances [17]. Kumar et al. [18] used different modelling approaches, namely regression, backpropagation neural network (BNN) and recurrent neural network (RNN), to predict different response variables of structural steels on hard turning for automotive applications. Usually, FMDP steels can be produced repeatedly by a typical intercritical annealing process [19-23]. The experimental techniques of the heat treatment route are covered as an essential way to confirm the formation of FMDP steel, say the two-phase microstructure. During heat treatment, it can be controlled by the considerations required to produce different volume fractions of the two or multi phases in the microstructure. Experimentally, DP steel with different martensite morphologies at various island volume fractions can be produced by a three-step intercritical annealing process [22-23]. During the intercritical annealing process, the specimen is initially heated to a specific range of temperatures, including the retention time, and placed in a muffle furnace with an argon environment. Different holding times and temperatures help for achieving different grain growth for a fine and a specific coarse island morphology. For subsequent movement, those test pieces are immediately located in a separate muffle furnace for an intercritical annealing stage at various temperatures. In the final step, the processed pieces are quenched directly into the water. The overall mechanical characteristics of the FMDP steels depend on their microstructures robustly. Thus, the modelling with proper sensitivity capabilities needs to be incorporated into a complex micro-structure environment.

From this standpoint, the micromechanics FE model is utilised to understand severe deformation mechanics, route of stress-strain partitioning and strain localisation due to heterogeneity [24-29]. The appearance of the peak nominal stress for the plastic materials is associated with the loss of stability of uniform deformation. The subsequent strain localisation leads to the situation of loss of uniform deformation, plastic instability and fracture in simple tension. Therefore, it indicates the damage initiation and propagation. In general, the plastic instability of the material can be considered in different ways in modelling. Mainly, it can be directed in the modelling as follows: (1) considering initial geometrical imperfections [30], (2) applying the theories of damage and void-growth [31-33], and (3) rising and reducing level inhomogeneity in the microstructure [24-27, 34]. Das et al. [35] studied the influence of parameters like ferrite grain size and its spatial distribution, size and fraction of island on the deformation at different strain rates. In this present work, flow behaviour, key plastic strain localisation settings and ductile failure mechanisms are studied via 2D-RVEs. Such a failure mechanism is predicted in the form of plastic strain localisation which arises due to the micro inhomogeneity present in the typical microstructure and its incompatible deformation between the island and ferritic-matrix. Furthermore, the influence of MVFs and orientations of islands in the microstructures on severe deformation are manifested.

MICROMECHANICAL INVESTIGATION

Constitutive Elucidation

In this computational investigation, individual ferrite and martensite of FMDP steel are represented in the Abaqus part model by means of micromechanics based RVE to comprehend the tensile deformation characteristics. Phase fractions such as 76.5% and 23.5% matrix-island FMDP 600 [24]; 90% and 10% matrix-island FMDP590 steels [36] are selected based on literature. In this work, two-dimensional representative volume elements (2D-RVEs) of microstructure are simulated. In 2D-RVEs, martensite-island are randomly distributed in the phase of ferritic-matrix. For 76.5 % matrix and 23.5% island [24], and 90% matrix and 10% island [36], steels flow curve is explained in Figure 1(a) and Figure 1(b), respectively and supplied in finite element simulation. By keeping the same modelling surroundings, 2D-RVEs have been created with 10-35% MVF to predict the volume fraction effect on the severity of the deformation trend. Additional criteria like the law of failure and damage are not incorporated in the present numerical investigation. A perfect bonding between two constituents (ferrite-martensite) in the microstructure is chosen for the simulation via 2D-RVEs in FE software. In the RVE model, von Mises yield criteria, associative flow rule and isotropic hardening rule can be taken for the island and matrix phase.

Consecutively, von Mises yield criteria, the stress-strain behaviour of each single-phase and isotropic hardening rule are considered for the current FE analysis in the micromechanical modelling of FMDP steel. To describe the isotropic hardening behaviour in every single phase in the calculations, the RVE model via a dislocation theory [36-37] has been used. Here, Eq. (1) explains the stress-strain field of soft-ferritic and hard-island phases.

$$\sigma^{f,m} = {\sigma_y}^{f,m} + \alpha M S \sqrt{b} \sqrt{\frac{1 - exp(-M k_r \varepsilon)}{k_r L}}^{f,m} \quad (1)$$

where stress ($\sigma^{f,m}$) is at the true strain of (ε), other significant specified material constants of FMDP steel in the model are used from the preceding study [36-37].

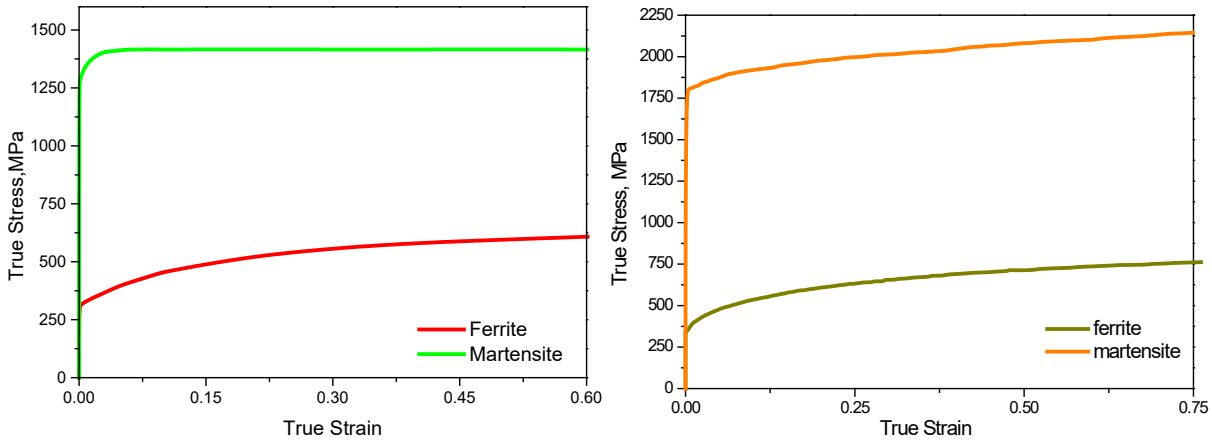

(a) (b)

Figure 1. Flow curves of each phase (ferritic-matrix and martensite-island) for (a) DP 600 and (b) DP 590 steel.

Expression of the 1st term in Eq. (1) is for the yield stress(σ_Y), and total contributions are friction stress, solid solution strengthening, precipitation strengthening with Nb, Ti, and/or V, grain-size, can be expressed as:

$$\sigma_y{}^{f,m} = 70 + 37\ wt.\%Mn + 83\ wt.\%Si + 2918\ wt.\%N_{sol} + 33\ wt.\%Ni - 30\ wt.\%Cr + 680\ wt.\%P + 38\ wt.\%Cu + 11\ wt.\ \%Mo + 5000\ wt.\%C + \frac{15.1}{\sqrt{d}} \quad (2)$$

In Eq. (2), the foremost term is friction stress. Friction stress ($\sigma_{F.S.}$) value is 70 MPa, and d (grain-size) is in mm. The average grain size is 10 μm. In the next term, the subsequent parameters that are intended for ferritic-matrix and island on the RVEs simulation are tabulated in Table 1.

Table 1. Explanation of the various materials parameters [36-37].

Parameters	Symbol	Value
Taylor constant	α	0.33
Taylor factor	M	3
Shear modulus	S	80,000 MPa
Burger's vector	b	2.5×10^{-10} m
Recovery rate in ferrite		$10^{-5}/d_\alpha$
Recovery rate in martensite	k_r	41
Dislocation mean free path for martensite	L	3.8×10^{-8} m

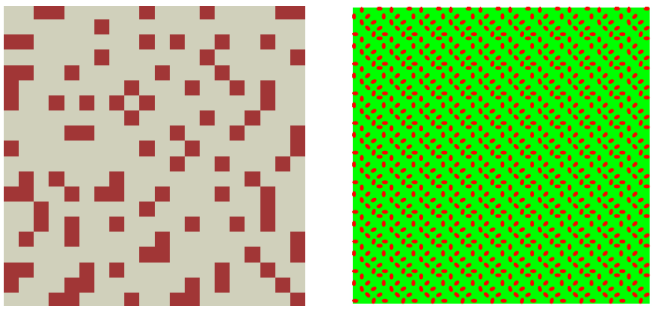

(a) (b)

Figure 2. 2D-RVEs model: (a) FMDP 600 steel, (b) FMDP 590 with binary microstructural constituents.

2D RVE Simulation

RVE geometrical models are represented in Figure 2. A random distribution of martensite in RVEs is modelled and analysed using the Abaqus 6.13 standard explicit code. The grey modules are ferrite, and brown modules are island constituents in the microstructure as shown in Figure 2(a). FMDP steels were considered in FE simulations. Initially, 2D RVE for 23.5% island (2-D RVE in μm^2: 100 × 100) and 10% island (2-D RVE in μm^2: 100 × 100) FMDP steel with different island position settings are integrated into the microstructure to check the prediction capability of the flow curve behaviour. The RVE of FMDP steel with a 10% island is shown in Figure 2(b). Here, elliptical morphology islands are

embedded in an arbitrary manner in the ferritic-matrix. The difference from the other model is the morphology of hard-island, average area of a martensite-island, and position settings. The average area of each island in FMDP steel (10% island) is 1.0μm^2, and the aspect ratio (AR) is 2.0. In the present study, the deformation characteristics are predicted by following the mechanical fields of individual phases in FMDP steels, hence the FE based 2D-RVEs.

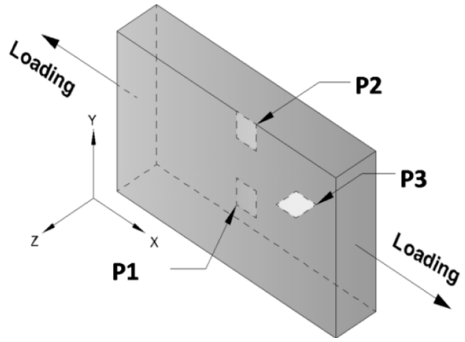

Figure 3. Altered positions of microelements, and following BCs, on a sheet specimen in monotonic loading.

These 2D-RVEs are the intended two-dimensional microstructure, where islands are aimlessly scattered in soft ferritic-matrix but with aimed orientations. The boundary condition and element type were altered according to the position of the representative elements in the microstructure of the specimen. Figure 3 illustrates three different situations of two-dimensional representative volume elements. Three microelements positions (in Figure 3) such as P1, P2 and P3 are identified on a sheet specimen under uniaxial tensile loading. The material in position P1 and P2, for these locations modelling with plain stress state, is considered. Since P1 and P2 located in the X–Y coordinate plane, the in-plane dimension of this tensile ductility test specimen is much larger than its thickness (t). So, the zero stress value in Z-direction can be considered. However, the lateral boundary conditions are different for P1 and P2. According to the element P1 in the tensile ductility sample, the BC on the lateral side is considered with zero movement in the Y path. As the lateral side of the P2 position is adjacent to the top, i.e., open boundary of the tensile ductility sample shown in Figure 3, it can be considered no constraint. Figure 4 shows the detailed schematic representations of BCs for position P2. The RVE of P3 is located on the plane of X–Z axis. Therefore, the condition of plain strain numerical modelling technique is considered because the width of the sheet specimen is much larger than its thickness. Further, no lateral boundary conditions (LBCs) are required because both the lateral sides of the position P3 are close to the free boundary. But in the case of P1, P2 and P3, the entire assigned nodes on the right side of the representative element of the microstructure have applied the displacement in the X-path. They are allowed to move with no restraint in Y-path, meanwhile a tensile deformation. In the X-direction, all nodes along the left side edge are fixed, but they are free to move in the Y-path.

RESULTS AND DISCUSSION

Engineering Flow Curve of DP Steel

A number of deformation plasticity issues are yet to be fully understood due to the complex nature of FMDP steels. This work aims to make out the complex characteristics of the automotive material through RVE modelling. Hence the average engineering strain in the X-path is obtained by the displacement of the right edge, i.e. numerator with the model original length as denominator of a particular numerical model. Average engineering stress is obtained by the ratio of reaction force (RF) of the same 2D-RVE in the X- path, i.e. numerator with an initial cross sectional area (i.e. denominator).

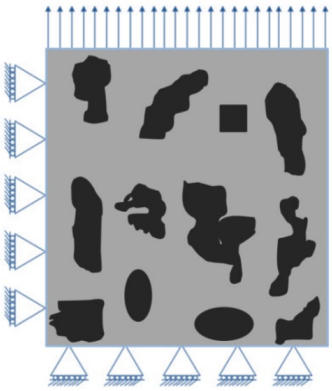

Figure 4. Details schematic representations of boundary condition.

The Abaqus software is used for computations of finite element results for examining the failure modes of the RVE. For P1 and P2 positions, plane stress elements (CPS3) are used. And for position P3, CPE3 plane strain elements are taken for the considered numerical model of FMDP-600, as in Figure 2(a). The experimental tensile flow curve of FMDP 600 and FMDP 590 steel are taken from the reference [24] and [36], respectively. The result of RVEs simulated data with experimental data are in reasonably well agreement in the engineering sense. The comparisons are shown in Figure 5 and Figure 6. Also, Figure 5 shows the comparison of flow curves between a random distribution and approximately real martensite distribution in the microstructure with experimental results. In both RVE simulations, no separate damage law is introduced. It clearly indicates from the RVE results (Figure 5) that a better prediction is observed for random distribution. Flow curve can be captured by the incorporating of material damage variable or geometrical imperfection or material imperfection. In the current study, material imperfection by the difference in stress-strain properties among phases is already available within the microstructure. In FMDP steel, flow properties of ferrite-matrix and island phases are different; therefore, material imperfection is present. Hence the random distribution of martensite-island closely matches with the experimental flow curve, as shown in Figure 5. This is possibly due to the averaging of dislocation movement in the plastic deformation since no separate damage law is introduced in the modelling.

For numerical analysis, displacement control mode in RVE simulations of FMDP 590 is considered. The bottom edge of RVE is constrained to move in Y-path and allowed to move in the X- path, while the left side is constrained to move in X-path and allowed to move in Y-path. All the nodes along the top side have the same movement in the Y-path. In this manifestation, the plane strain elements were preferred for meshing two-dimensional RVE of FMDP-590 steel. The overall macro-scale engineering stress is determined by the reaction force (RF) in the Y-path divided by the initial cross-sectional region, i.e. the initial thickness. Overall macroscopic engineering strain in the Y-path is obtained by dividing the displacement of the top edge, i.e. numerator with the original length of the model as the denominator.

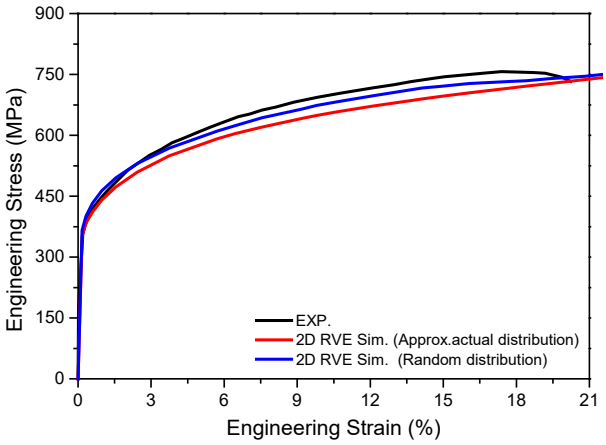

Figure 5. Comparison of the macroscopic stress-strain curves with actual and random 2D RVEs simulation vs. experimental curve.

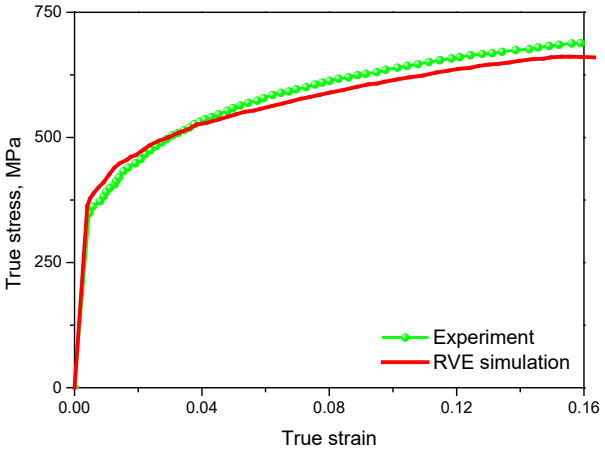

Figure 6. Flow curves relationship between experiment and simulation of FMDP 590 steel.

Failure Mechanisms Analysis

DP 600 steel can be considered for a typical automotive wheel disc and is one of the most severely stressed mechanisms in the vehicle, where its durability is of vital importance regarding human safety [38]. A comprehensive two-scale micromechanical modelling through the RVE strategy is also used for the study to determine the failure characteristics of FMDP steels due to the tensile load acting on them. Uniaxial tensile flow behaviour of the investigated

FMDP 600 steel is explored extensively. Also, the same modelling procedure has been kept for the investigation of island morphology and orientation effect from the natural fallout of plastic equivalent strain (PEEQ) and von Mises equivalent stress distribution by 2D-RVE. Different average strains have been applied on the RVE of positions P1, P2 and P3. The results of the failure mechanisms are portrayed in Figure 7 and Figure 8 accordingly. A predominant shear failure mechanism is characterised by the RVE simulation under uniaxial tensile loading (UTL) for position P2. The plastic flow behaviour on position P2 in the form of equivalent plastic strain localisation is addressed in Figure 7 P-2(a) and Figure 7 P-2(b). The higher stress concentration regions for a rising strain are also demonstrated in Figure 8 P-2(a) and Figure 8 P-2(b). It can be observed that the local failure mechanisms are closely related to the stress state in the FMDP steel.

Hence, this is clear from the above results that mainly, the matrix is forced to follow the yielding in the microstructure during the early stages of straining, while the second phase-islands continue to carry higher stresses. Thus the deformation is being mismatched, and it gradually decreases the partitioning of strain deformation. Typically it is significant to be found that the plastic strain localisation lies in the RVEs, mainly in the ferrite grains and their grain boundaries. Only rarely does the macroscopic shear band cross through some neck regions in martensite grains. Owing to geometrical discontinuity in metal, Rana et al. [39] showed the consequence of stress field due to isotropic material inhomogeneity in structural metal under monotonic tensile stress for soft and hard inclusions by developing numerical models. Such a geometrical discontinuity or stress concentrator produces a rise of local stresses within the component. There is a stress concentration in the vicinity of these discontinuities. This plastic deformation or yielding is local and restricted to a very small region in the material. The presence of such an unavoidable notch or stress concentrator is the source of crack initiation due to a high rise of stress concentration, thereby leading to early failure of the components.

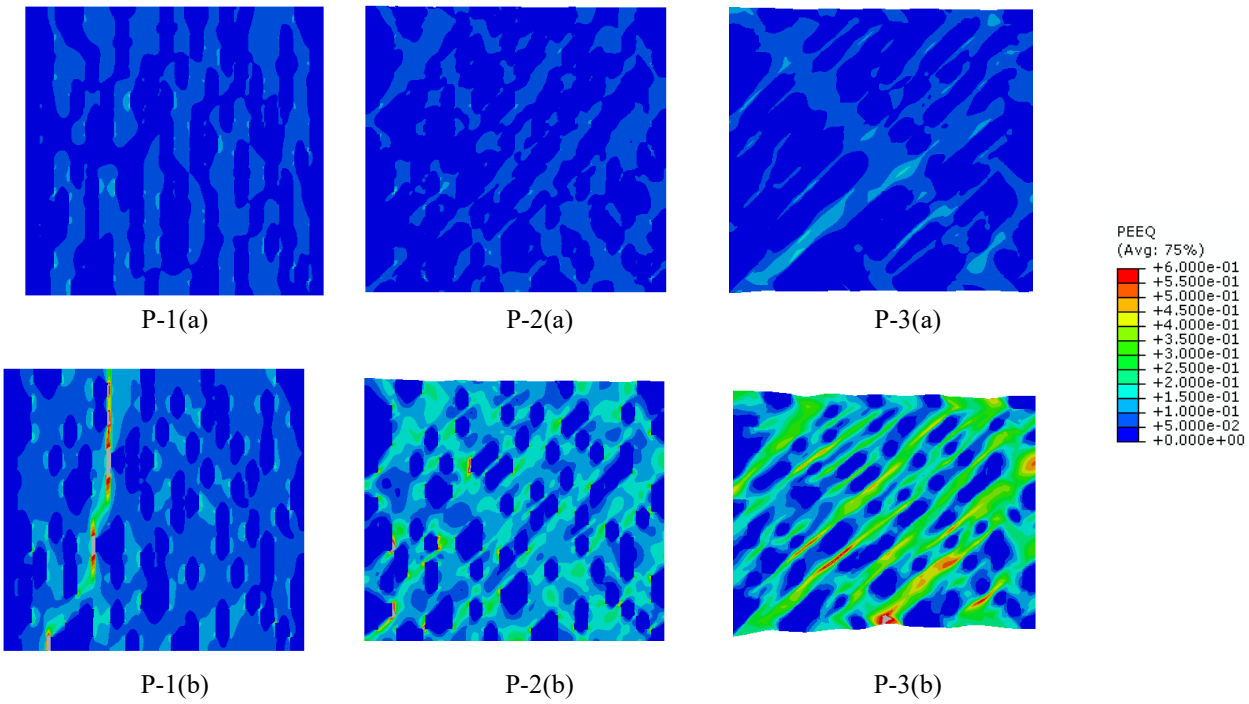

Figure 7. Dispersal of equivalent plastic strain in 2D-RVE on P1, P2 and P3positions under monotonic loading: on P-1 engg. strain (%) of (P-1.a) 3.5%, (P-1.b) 6%; on P-2 engg. strain (%) of (P-2.a) 3.5%, (P-2.b) 10%; and on P-3 engg. strain (%) of (P-3.a) 3.5%, (P-3.b) 14%.

At various aggregate strain levels during elastic-plastic deformation, the highest equivalent plastic strain initiates to localise the shear band at an engineering strain ($\varepsilon_{avg.}$) of 10%, which is shown in Figure 7 P-2 (a) and P-2 (b). This can lead to the final shear band failure in the next 1-3% overall strain. That means only one dominant shear band in the RVEs (i.e. failure trend) can lead to the final failure of the FMDP steel at more than 10% engineering strain. Detail examinations of numerical RVE show that severe plastic strain localisation appears mainly in the matrix regions of the simulated micro-model. Different failure modes are observed depending on the location of the element. Here the vertical split failure mechanism perpendicular to the loading direction is indicated at P1. At 6% engineering strain, an instability based failure mechanism is observed at P1 with less overall material ductility than other locations. This prediction is manifested in Figure 7 P-1(a) and P-1 (b) and Figure 8 P-1(a) and P-1(b) correspondingly.

An RVE result of considerable thinning at P3 along the width is indicated at an overall strain level of 14%. It is similar to the experimental observation of the sample through thickness thinning failure trend presented by Sun et al. [25]. This significant mechanism can be observed in Figure 7 P-3(b) and Figure 8 P-3(b). The most important factor of this severe deformation pattern and failure directions is that the plastic deformation localisations were occurring mainly within the ferritic-matrix; grow and coalesce, and eventually form various sizes of deformation bands. Then islands inside the deformation bands also deform heavily. Such a mechanism of deformation band results concentrated high rate deformation mainly within the deformation band, and thus cause an unloading consequence in other areas.

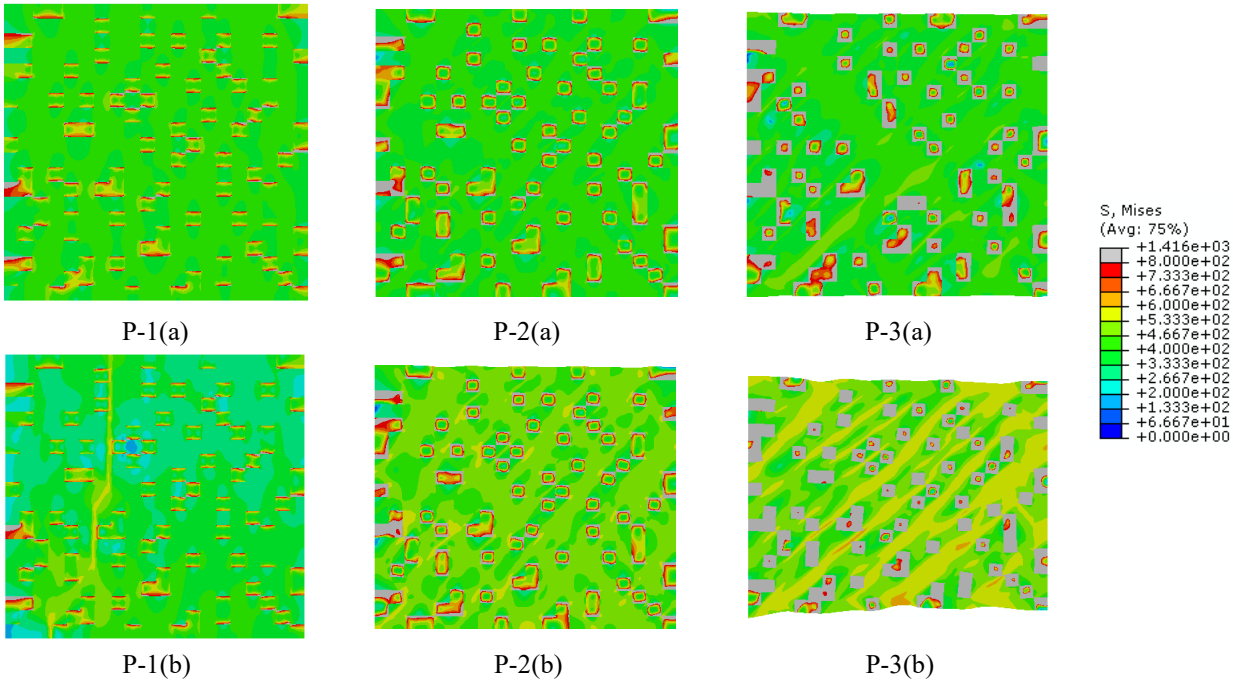

Figure 8. Dispersal of equivalent plastic stress state in 2D-RVE on P1, P2 and P3 positions under monotonic loading: on P-1 engg. strain (%) of (P-1.a) 3.5%, (P-1.b) 6%; on P-2 engg. strain (%) of (P-2.a) 3.5%, (P-2.b) 10%; and on P-3 position engg. strain (%) of (P-3.a) 3.5%, (P-3.b) 14%.

Recently, Ghosal et al. [40] and Ghosal and Paul [41] explored the influence of pre-straining on the monotonic behaviour of DP 600 steel. The same group [40-42] also determined a number of tensile properties, which are considered from the overall flow curve such as the yield strength (YS), ultimate tensile strength (UTS), uniform elongation (UEL), and total elongation (TEL). In the present study, the final failure mechanisms predicted under uniaxial loading with distinct BC are in good agreements with experimental observations and real microstructure modelling reported by Sun et al. [25] and Paul and Kumar [36]. Here 2D RVE is used, which looks like a data matrix or QR code. Figure 9 shows an equivalent plastic strain and a von Mises stress distribution during 10% engineering straining, where elliptical martensite morphology is embedded in ferrite matrix having 10% MVF and 0º, 15º, 30º, 45º, 60º, 75º, 90º martensite orientations. Currently Rana et al. [42] showed that the deformation band localisation modes could alter from inclined to perpendicular of the DP steel. As a consequence, it is fractured in a perpendicular or inclined manner. Similarly, the stress state of the sheet metal varies during forming operation, and failure can be different in those cases.

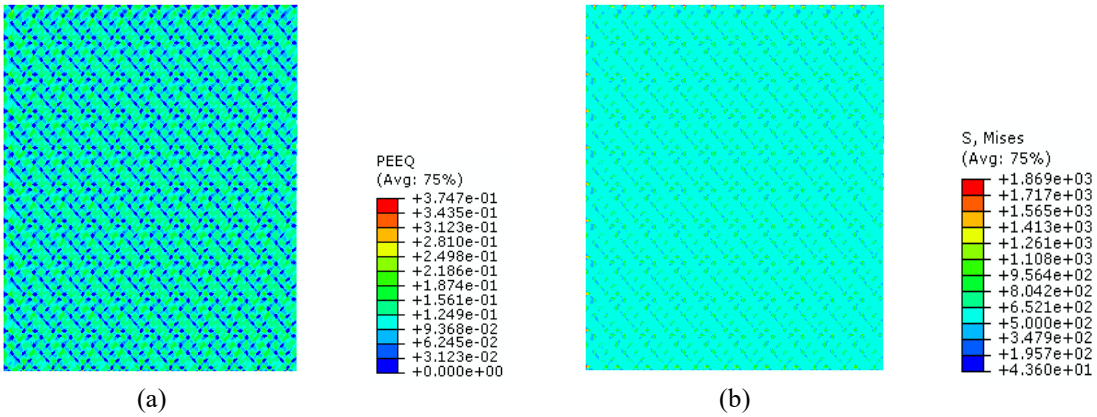

Figure 9. In the course of a 10.0% Engineering straining: deformation fashion (a); and equivalent plastic stress dispersal (b) of FMDP-590 (10% MVF and having 0º,15º,30º,45º,60º,75º, 90º martensite orientations).

Influence of Volume Fraction and Orientation

The influence of MVF in monotonic deformation mechanisms of FMDP steel is studied for a mostly applied range of phase fractions such as 10%, 23.5%, 27% and 35% MVF in a matrix. The distribution of the equivalent plastic strain at an overall engineering strain (εavg.) of 10% for the said MVFs is revealed in Figure 10. The distribution of equivalent stress-strain results clearly shows that the inhomogeneous plastic deformation is cropped up in all the microstructure of FMDP steels. But the severe localised deformation raised with a rising MVF. In most cases, the stress states in the ferritic phase are almost close to each other. On the other hand long localisation deformation bands appear with a rise of MVF.

These bands are mainly found in the pliable phase (ferritic-matrix) irrespective of the MVFs. The role of island morphology orientation on the severe deformation behaviour of the FMDP steels is also addressed.

However, a number of island orientations issue in DP steels are yet to be fully demonstrated computationally due to their complex microstructure. Moreover, Figure 9 illustrates the von Mises stress state considering 0º and 90º orientations of islands. While Figure 11 represents the equivalent plastic strain and Mises stress, S state without considering 0º and 90º orientation of the island phase. Figure 12 shows the comparison of equivalent plastic strain (PEEQ) and Mises stress, S state with and without having 0º and 90º islands orientations along the loading path during 10% engineering straining. Thus it is observed that the same loading condition may lead to different interpretations of the severe stress state in the microstructure depending upon the orientation of the martensite-islands. All elements are considered to have the same grain size in a 2D-RVE. Hence element size is taken constant in all the RVEs to avoid the mesh size influence. The grain boundary hardening can slightly delay the initiation of plastic strain localisation in the RVE. Figure 6 shows the prediction of the flow curve with various elliptical martensite orientations. Whereas in Figure 5, it's depicted that random distribution and orientation predict well. Hardly change in numerical value may be found without a noticeable change in trend considering the failure criterion. However, in the present investigation, the main interest lies upon the overall plastic flow behaviour, failure mechanisms and severe deformation localisation of the material. So the current RVEs simulation will be provided for the purpose of this study.

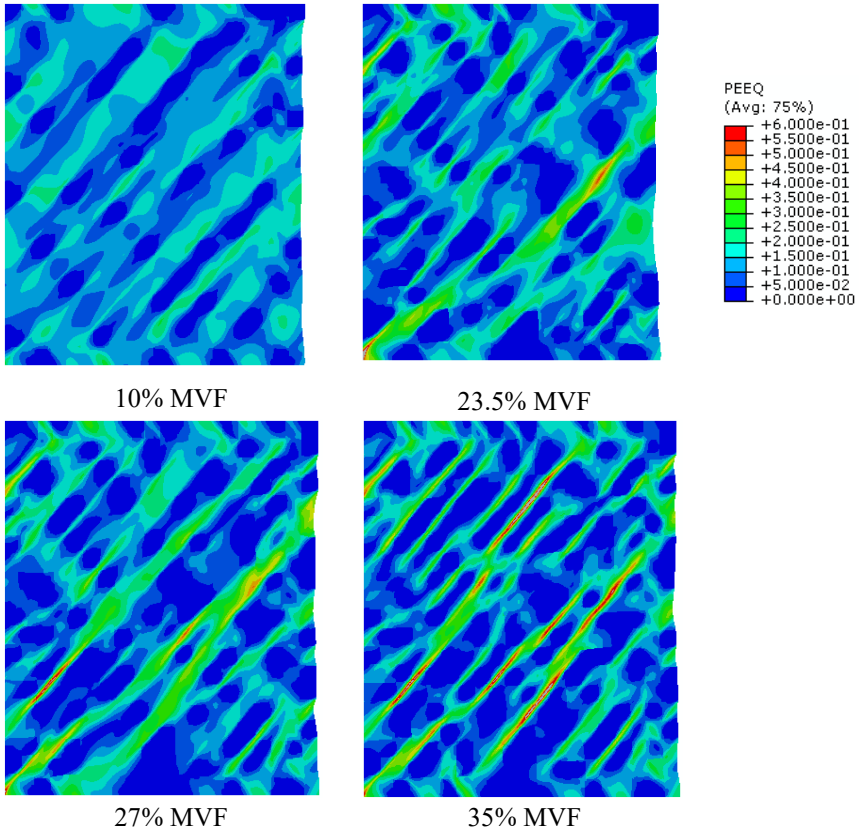

Figure 10. During 10.0% Engineering straining, deformation pattern of FMDP steel with various MVF.

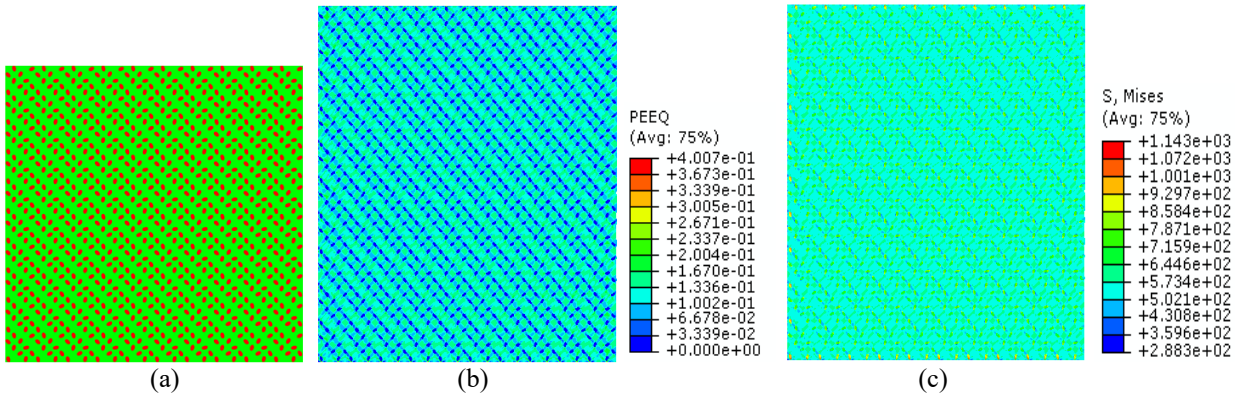

Figure11. In the course of a10% engineering straining: (a) RVE (without 0º and 90º islands orientations in loading path), (b) equivalent plastic strain distribution and (c) von Mises stress state dispersal of FMDP 590

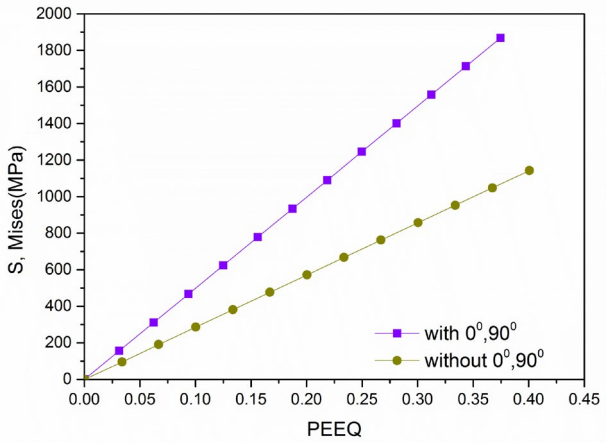

Figure12. In the course of a 10% engineering straining ($\varepsilon_{avg.}$); comparison of PEEQ Vs. S, Mises stress variation with and without having 0º and 90º islands positions along loading path.

Failure mechanisms and strain deformation comparison for FMDP steels is discussed and tabulated. These results suggest; (a) the failure mechanism causes due to microstructural inhomogeneity, (b) indication of the failure pattern throughout the cross-section with (i) detailed insight in the process of plastic localisation by prominent shear band localisation at position P2, (ii) the local stress-strain fields in the microstructure create vertical split failure mechanisms perpendicular to the load setting path at position P1 and, (iii) diminishing width of RVE at position P3. All observed failure patterns from the current RVEs are similar with the local failure shown from the tensile test experiment reported by Sun et al.[25]. Table 2 shows the comparative result of failure strain (onset of plastic instability). On the other hand, the ductile failure modes of carbon steel material are established in the form of fracture instability and plastic collapse condition [43].

Table 2. Comparison of failure strain (plastic instability started).

Failure pattern	DP steel		
	DP600 (RVE simulation)	DP590 [36]	DP980 [25]
Dominant shear failure	10	17.5	11.5
Split	6	6.5	3.2
Necking(thickness thinning)	14	17.5	22.4

From the results in Figure 9, Figure 11 and Figure 12, it has been shown that the microstructure without allowing for 0º and 90º orientations of islands has produced less maximum severe stress in the identical load setting. The results also explained the influence of island shapes and orientations on plastic behaviour, and local mechanical fields of the material. One of the reasons for this is that after the localisation of deformation, the local mechanical fields of the deformation depend on the morphology and orientation of islands adjacent to the localised deformed region. Other reasons may have a trend of larger strain hardening capacity with 00, 450 and 900 compared to other considered orientations. This may be due to higher ductility for the orientation of 450 compared to 00 and 900. In the case of tensile strength, it shows the opposite tendency. Furthermore, the strain partitioning is responsible for inhomogeneous strain distribution within the FMDP steel. The partitioning of stress (i.e. high stress carried by the island phase in comparison to ferritic phase) between phases is also responsible for the development of a severe stress field and consequently inhomogeneous deformation, severe deformation localisation and fracture failure.

CONCLUSION

The deformation behaviour of FMDP steels under monotonic loading can be predicted using FE simulation via 2D RVEs, a multiscale computational scheme. The present modelling describes the deformation localisation and local stress state variations in the FMDP steels. From this investigation the following key conclusions can be made as:

i. Elasto-plastic finite element analysis is performed on the 2D-RVE models for microstructures to predict the engineering stress–strain behaviour under monotonic loading. Therefore, the plasticity model consisting of isotropic von Mises yield surface, with an associated flow rule, is able to describe the macroscopic plasticity behaviour of the material.
ii. Such modelling can predict the failure mode (ductile) subjected to the different boundary conditions using 2D-RVE of the complex microstructure. Mainly initial microstructural non uniformity among the various constituent phases causes plastic instability. It is predicted in the form of plastic strain localisation resulting from the ill-assorted deformation behaviour between two phases.

iii. Effect of severe stress fields with phase fraction, hence island in FMDP steels, is explored. Even for same level of straining, for example, 10% average engineering strain, the deformation inhomogeneity rises with a reducing ferritic-matrix volume fraction in FMDP steel.

iv. Influence of severe stress fields with various island orientations, von Mises stress and plastic equivalent strain distribution were examined. Results indicate that more strain localisation zone can be observed in the case of 0º and 90º island positions with loading direction and can be considered as early fracture-failure.

v. The result shows that the centre of the tensile specimen fractured in a perpendicular manner, while the inclined fracture is observed on both sides. Similarly, the stress state of the sheet metal varies during forming operation, and failure can be different in those cases.

vi. However, the current numerical study is aimed at achieving results through simplified RVE modelling. This method is intended to be as popular as the conventional method for determining such a complex material characteristics. Finally, such a complex stress-strain field in a FMDP steel is derived successfully in the engineering sense by this investigation. Moreover, for improvement, the interface and interphase damage behaviour also may be integrated into the proposed numerical approach by unifying any separate damage law or failure criteria. For this purpose, minor change in numerical value may be found without alteration in the revealed trend.

ACKNOWLEDGEMENT

This work was carried out with the support of Indian Institute of Engineering Science and Technology, Shibpur. A.K. Rana is also thankful to The ICFAI University Tripura for providing the environment to do the later necessary works.

REFERENCES

[1] Belgasam TM, Zbib HM. Key factors influencing the energy absorption of dual-phase steels: multiscale material model approach and microstructural optimisation. Metallurgical and Materials Transactions A 2018; 49: 2419–2440.

[2] Uthaisangsuk V, Prahl U, Bleck W. Modelling of damage and failure in multiphase high strength. Engineering Fracture Mechanics 2011; 78(3): 469-486.

[3] Belgasam TM., Zbib HM. Microstructure optimisation of dual-phase steels using a representative volume element and a response surface method: Parametric study. Metallurgical and Materials Transactions A 2017; 48(12): 6153-6177.

[4] Sirinakorn T, Wongwises S, Uthaisangsuk V. A study of local deformation and damage of dual phase steel. Materials and Design 2014; 64: 729–742.

[5] Rana AK, Paul SK, Dey PP. Effect of martensite volume fraction on strain partitioning behavior of dual phase steel. Physical Mesomechanics 2018; 21(4): 333-340.

[6] Rana AK, Paul SK, Dey PP. Effect of martensite volume fraction on cyclic plastic deformation behavior of dual phase steel: micromechanics simulation study. Journal of Materials Research and Technology 2019; 8(5):3705-3712.

[7] Paul SK. Effect of martensite volume fraction on stress triaxiality and deformation behavior of dual phase steel. Materials and Design 2013; 50: 782-789.

[8] Bag A, Ray KK, Dwarakadasa ES. Influence of martensite content and morphology on tensile and impact properties of high-martensite dual-phase steels. Metallurgical and Materials Transactions A 1999; 30(5): 1193-1202.

[9] Paul SK, Mukherjee M. Determination of bulk flow properties of a material from the flow properties of its constituent phases. Computational Materials Science 2014; 84: 1-12.

[10] Sun S, Pugh M. Properties of thermomechanically processed dual-phase steels containing fibrous martensite, Materials Science and Engineering A 2002; 335: 298-308.

[11] Byun TS, Kim IS. Tensile properties and inhomogeneous deformation of Ferrite–Martensite dual-phase steels. Journal of Materials Science 1993; 28: 2923-2932.

[12] Ososkov Y, Wilkinson DS, Jain M, Simpson T. In-situ measurement of local strain partitioning in a commercial dual-phase steel. International Journal of Materials Research 2007; 98(8): 664-673.

[13] Kang J, Ososkov Y, Embury JD, Wilkinson DS. Digital image correlation studies for microscopic strain distribution and damage in dual phase steels. ScriptaMaterialia 2007; 56(11): 999-1002.

[14] Korzekwa DA, Matlock DK, Krauss G. Dislocation substructure as a function of strain in a dual-phase steel. Metallurgical Transactions A1984; 15(6): 1221-1228.

[15] Jia N, Cong ZH, Sun X, et al. An in situ high-energy X-ray diffraction study of micromechanical behaviour of multiple phases in advanced high-strength steels. Acta Materialia 2009; 57(13): 3965-3977.

[16] Cong ZH, Jia N, Sun X, Ren Y, et al. Stress and strain partitioning of ferrite and martensite during deformation. Metallurgical and Materials Transactions A 2009; 40(6): 1383-1387.

[17] Kamal MRM, Bazilah NF, Pzil NFM, et al. Effect of plunger speed and solid fraction on automotive component by thixoforming simulation. International Journal of Automotive and Mechanical Engineering 2020; 17(2): 7942 – 7955.

[18] Kumar R, Modi A, Panda A, et al. Hard turning on JIS S45C structural steel: an experimental, modelling and optimisation approach. International Journal of Automotive and Mechanical Engineering 2019; 16(4): 7315-7340.

[19] Davies RG. Influence of martensite composition and content on the properties of dual phase steels. Metallurgical Transactions A 1978; 9(5): 671-679.

[20] Basu P, Acharyya SK, Sahoo P. A correlation study between mechanical properties and morphological variation of 20MnMoNi55 steel. Silicon 2018; 10 (4): 1257-1264.

[21] Klaar HJ, El-Sesy IA, Hussein AHA. Microstructure and properties of a C–Mn–Si–dual-phase steel. Steel Research 1990; 61(2): 85-92.

[22] Paul SK, Stanford N, Hilditch T. Effect of martensite volume fraction on low cycle fatigue behaviour of dual phase steels: Experimental and microstructural investigation. Materials Science & Engineering A 2015; 638: 296-304.

[23] Paul SK, Stanford N, Hilditch T. Effect of martensite morphology on low cycle fatigue behaviour of dual phase steels: Experimental and microstructural investigation. Materials Science & Engineering A 2015; 644: 53-60.

[24] Wei X, Asgari SA, Wang JT, Rolfe BF, Zhu HC, Hodgson PD. Micromechanical modelling of bending under tension forming behaviour of dual phase steel 600. Computational Materials Science 2015; 108: 72-79.

[25] Sun X, Choi KS, Liu WN, Khaleel MA. Predicting failure modes and ductility of dual phase steels using plastic strain localization. International Journal of Plasticity 2009; 25(10): 1888-1909.

[26] Sun X, Choi KS, Soulami A, Liu WN, Khaleel MA. On key factors influencing ductile fractures of dual phase (DP) steels. Materials Science & Engineering A 2009; 526(1-2): 140-149.

[27] Choi KS, Soulami A, Liu WN, Sun X, Khaleel MA. Influence of various material design parameters on deformation behaviors of TRIP steels. Computational Materials Science 2010; 50(2): 720-730.

[28] Marciniak Z, Kuczynski K. Limit strains in the processes of stretch-forming sheet metal. International Journal of Mechanical Science 1967; 9 (9): 609-612.

[29] Uthaisangsuk V, Prahl U, Bleck W. Stretch-flangeability characterisation of multiphase steel using a microstructure based failure modelling. Computational Materials Science 2009; 45(3): 617-623.

[30] Gurson AL, Plastic flow and fracture behaviour of ductile materials incorporating void nucleation, growth and coalescence. PhD Thesis, Brown University, USA, 1975.

[31] TvergaardV. On localization in ductile materials containing spherical voids. International Journal of Fracture 1982; 18: 237-252.

[32] Tvergaard V, Needleman A. Analysis of the cup–cone fracture in a round tensile bar. Acta Metallurgica 1984; 32 (1): 157-169.

[33] Ramazani A, Mukherjee K, Schwedt A, et al. Quantification the effect of transformation-induced geometrically necessary dislocations on the flow curve modelling of DP steels. International Journal of Plasticity 2013; 43: 128-152.

[34] Chatzigeorgiou G, Charalambakis N. Instability analysis of non-homogeneous materials under biaxial loading. International Journal of Plasticity 2005; 21 (10): 1970-1999.

[35] Das A, Tarafder S, Sivaprasad S,Chakrabarti D. Influence of microstructure and strain rate on the strain partitioning behaviour of dual phase steels. Materials Science and Engineering A 2019; 754: 348-360.

[36] Paul SK, Kumar A. Micromechanics based modelling to predict flow behavior and plastic strain localization of dual phase steels. Computational Materials Science 2012; 63: 66-74.

[37] Paul SK. Real microstructure based micromechanical model to simulate microstructural level deformation behavior and failure initiation in DP 590 steel. Materials and Design 2013; 44: 397-406.

[38] Das B, Paul SK, Singh A, Arora KS, Shome M, The effect of thickness variation and pre-strain on the cornering fatigue life prediction of a DP600 steel wheel disc. International Journal of Fatigue 2020 139: 105799.

[39] Rana AK, Paul SK, Dey PP. Stress field in an isotropic elastic solid containing a circular hard or soft inclusion under uniaxial tensile stress. Materials Today: Proceedings 2019; 11: 657-666.

[40] Ghosal P, Paul SK, Das B, Chinara M, Arora KS. Notch fatigue performance of DP600 steel under different pre-straining paths. Theoretical and Applied Fracture Mechanics 2020; 108:102630.

[41] Ghosal P, Paul SK. Effect of specimen orientation to the rolling direction on uniaxial tensile forming and failure limits. Proceedings of the Institution of Mechanical Engineers, Part B: Journal of Engineering Manufacture 2020; 234(13):1598-1603.

[42] Rana AK, Paul SK, Dey PP. Effect of individual phase properties and volume fractions on the strain partitioning, deformation localization and tensile properties of DP steels. Sadhana 2020; 45:235.

[43] Rana AK, Acharyya SK, Dhar S. A simplified procedure to prediction of ductile failure modes of a SA333 Gr. 6 carbon steel pipe: Fracture instability and Plastic collapse condition. Materials Today: Proceedings 2019; 18: 2893-2902.